Gas Chromatography Plasma-Assisted Reaction Chemical Ionization Mass Spectrometry for Quantitative Detection of Bromine in Organic Compounds

ARTICLE *in* ANALYTICAL CHEMISTRY · JULY 2014

Impact Factor: 5.64 · DOI: 10.1021/ac501964u · Source: PubMed

5 AUTHORS, INCLUDING:

Kaveh Kahen
PerkinElmer
20 PUBLICATIONS **295** CITATIONS
SEE PROFILE

Hamid Badiei
PerkinElmer
23 PUBLICATIONS **189** CITATIONS
SEE PROFILE

analytical chemistry

Article

pubs.acs.org/ac

Gas Chromatography Plasma-Assisted Reaction Chemical Ionization Mass Spectrometry for Quantitative Detection of Bromine in Organic Compounds

Ninghang Lin,[†] Haopeng Wang,[†] Kaveh Kahen,[‡] Hamid Badiei,[‡] and Kaveh Jorabchi*[,†]

[†]Department of Chemistry, Georgetown University, Washington, DC 20057, United States

[‡]PerkinElmer Inc., Woodbridge, Ontario L4L8H1, Canada

Supporting Information

ABSTRACT: We have recently introduced plasma-assisted reaction chemical ionization mass spectrometry (PARCI-MS) for elemental analysis of halogens in organic compounds. Here, we utilize gas chromatography (GC) coupled to PARCI-MS to investigate the mechanism of Br^- ion generation from organobromines and to evaluate analytical performance of PARCI for organobromine analysis. Bromine atoms in compounds eluting from GC are converted to HBr in a low-pressure microwave induced helium plasma with trace amounts of hydrogen added as a reaction gas. Ionization is achieved by introducing nitrogen into the afterglow region of the plasma, liberating electrons via penning ionization and leading to formation of negative ions. We demonstrate that N_2 largely affects the ionization process, whereas H_2 affects both the ionization process and in-plasma reactions. Our investigations also suggest that dissociative electron capture is the main ionization route for formation of Br^- ions. Importantly, GC-PARCI-MS shows a uniform response factor for bromine across brominated compounds of drastically different chemical structures, confirming PARCI's ability to quantify organobromines in the absence of compound-specific standards. Over 3 orders of magnitude linear dynamic range is demonstrated for bromine quantification. We report a detection limit of 29 fg of bromine on-column, ~4-fold better than inductively coupled plasma-MS.

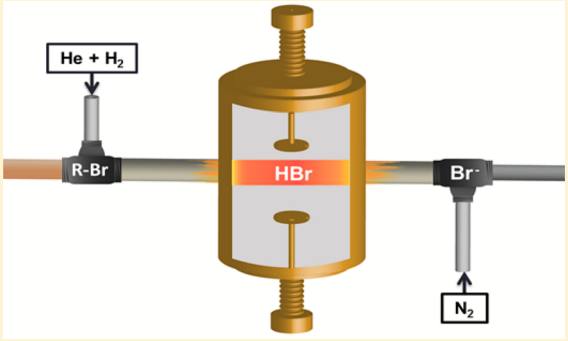

There has been an increasing concern in the last two decades for the presence of organobromines in the environment. These compounds appear among fire-retardants[1,2] and have a tendency to bio-accumulate, causing health problems such as neurotoxicity observed from polybrominated diphenyl ethers.[3,4] Moreover, organobromines are used as active pharmaceutical compounds and may also form as toxic impurities in pharmaceutical products.[5,6] Therefore, analytical techniques for detection, identification, and quantification of brominated organic compounds have received considerable attention.

High sensitivity and selectivity make mass spectrometric methods appealing for trace analysis of organobromines. Techniques such as atmospheric-pressure chemical ionization mass spectrometry (APCI-MS),[7,8] electrospray ionization (ESI)-MS,[9,10] and electron impact ionization (EI)-MS[11,12] have been used in organobromine detection and identification. Quantification and isotopic analysis in these methods, however, require individual standards for each species because of compound-dependent ionization. The ability to quantify in the absence of compound-specific standards is particularly important when new compounds are detected at trace levels. Environmental screening and metabolite quantification in early drug development are two examples of such studies.[2,9,13]

Elemental MS offers quantitative analysis in the absence of compound-specific standards. To preserve molecular information, a separation method is used prior to elemental MS. This methodology has been gaining significant attention via application of inductively coupled plasma (ICP)-MS to quantify heteroatoms (particularly P, S, Se, and As) in environmental and biological samples.[14−16]

Analysis of halogenated compounds by ICP-MS, however, is challenging because of low sensitivity of ICP-MS for halogens. This shortcoming arises from fundamental limitations in ionization and ion sampling particular to ICP-MS. In a typical argon ICP-MS, elements are ionized in positive mode. The high ionization potential of halogens limits the ionization efficiency for these elements (~5% for Br).[17] Moreover, the large argon ion current from the plasma creates a significant space charge effect, reducing analyte ion transmission into the mass analyzer.[18] Despite these limitations, the quantitative potential of elemental MS is demonstrated for organobromines using ICP-MS coupled to gas chromatography (GC) and liquid chromatography.[12,19−24] Interestingly, higher sensitivities have

Received: May 27, 2014
Accepted: July 8, 2014
Published: July 8, 2014

   dx.doi.org/10.1021/ac501964u | *Anal. Chem.* 2014, 86, 7954−7961

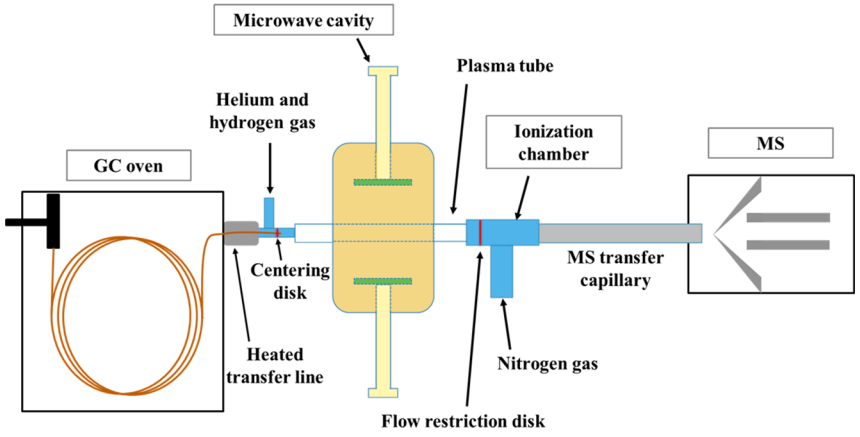

Figure 1. Schematic drawing of the gas chromatography plasma-assisted reaction chemical ionization mass spectrometry (GC-PARCI-MS).

Table 1. GC Program for Organobromine Analysis

temperature program	analytical performance	fundamental investigations
injector	230 °C	230 °C
transfer line	200 °C	200 °C
GC oven	35 °C (hold 2 min)	35 °C (hold 2 min)
	50 °C/min to 200 °C (hold 2 min)	15 °C/min to 45 °C (hold 3.5 min)
		30 °C/min to 150 °C (hold 0 min)
		50 °C/min to 200 °C (hold 0.5 min)

been reported in detection of polybrominated diphenyl ethers using ICP-MS compared to negative mode chemical ionization-MS and electron impact ionization-MS.[25,26] Compound-dependent ionization efficiencies in molecular ionization methods make sensitivity comparison between ICP-MS and other mass spectrometric methods difficult to generalize. However, the studies discussed above demonstrate that elemental MS has the potential to offer superior sensitivity in addition to excellent quantification for detection of halogenated organic compounds.

In recent years, dielectric barrier discharges (DBDs) have also gained attention for elemental and molecular analysis.[27] The use of these plasmas as ion sources has generally been limited to molecular ionization in ambient mass spectrometry.[27,28] Application of DBDs for element-selective detection of organohalogens online with gas chromatographic separations has been explored using atomic absorption,[29] molecular emission,[30] and chemilumenscence[31] spectroscopies. Note that molecular emission and chemiluminescence detectors provide compound-dependent response factors. A capacitively coupled microplasma has also been investigated as an excitation source for atomic emission spectroscopy[32] as well as an ion source for formation of negative halogen ions from organohalogens separated by GC.[33] For bromine detection, however, these methods have not provided a performance improvement over ICP-MS.

In view of the fundamental limitations of ICP-MS discussed above, we recently introduced plasma-assisted reaction chemical ionization (PARCI) to improve the sensitivity for elemental halogen detection from organohalogens.[34] The ion generation is fundamentally different in this approach compared to ICP. In PARCI, a low-pressure helium plasma serves as a reaction chamber to convert halogen atoms in organic compounds into small neutral molecules. Ionization occurs downstream of the plasma in negative mode by electrons released from penning ionization of a gas such as nitrogen.[34] Using flow injection analysis of aqueous organobromine solutions, we demonstrated 5−8 times higher sensitivity for PARCI-MS compared to ICP-MS. However, compound-dependent sensitivities were observed as a result of desolvation in the sample introduction system. The desolvation was necessary to reduce the solvent load into the plasma, which may cause deterioration of plasma temperature.

In the current study, we use gas chromatography to introduce the samples into PARCI-MS. This approach minimizes sampling biases and allows the characterization of fundamental aspects of ion generation in PARCI. The analytical performance of GC-PARCI-MS including dependence of response factor on the chemical structure of the analytes, linear dynamic range, and detection limits are also evaluated for organobromines.

EXPERIMENTAL SECTION

Instrumentation. A schematic drawing of the GC-PARCI-MS is presented in Figure 1. The apparatus is similar to the one reported earlier,[34] except that GC is used as the sample introduction system. Each component is briefly described below.

Gas Chromatography and Coupling to PARCI. A Star 3400CX gas chromatograph (Varian, Palo Alto, CA, United States) with a split injector and a capillary column (DB-5MS; 30 m × 0.250 mm, 0.25 μm film thickness; Agilent, Santa Clara, CA, United States) is utilized for sample introduction. The GC column is inserted through a heated transfer tube (200 °C) connected to a Swagelok tee upstream of the PARCI. The column is centered using a disk with a 1 mm i.d. in the downstream side of the tee. The plasma gas (He) and reactant gas (H_2) are introduced into the Swagelok tee, sweeping the GC eluents into the plasma.

The GC injector is operated at 230 °C with a split ratio of 50:1. High purity helium is used as the carrier gas at a flow rate of 1.7 mL/min through the column. During analysis, 0.5 μL

dx.doi.org/10.1021/ac501964u | Anal. Chem. 2014, 86, 7954−7961

analyte solutions are manually injected using a 5 μL GC syringe (Hamilton, Reno, NV, United States). The GC operating parameters are listed in Table 1.

PARCI-MS. Briefly, PARCI consists of a microwave induced plasma and an ionization chamber. The plasma is sustained in an alumina tube (6.35 mm o.d., 4.00 mm i.d., 10.16 cm length) inserted through a brass microwave cavity. A net power of 50 W supplied by a microwave power supply (MPG-4M, Opthos Instruments, Rockville, MD, United States) is used throughout the studies to maintain the plasma. To prepare the plasma gas mixture, ultrahigh purity grade H_2 is mixed into a constant flow of high purity helium (2.2 L/min controlled by Matheson 603 flow meter, Basking Ridge, NJ, United States) through a 100 μm i.d. fused silica capillary (75 cm in length). The flow rate of the reactant gas (H_2) is controlled by adjusting the pressure at the upstream end of the capillary. Flow of hydrogen at various pressure settings is measured off-line by tracking the movement of a soap bubble within a 2 mL pipette (Fisherbrand, Pittsburgh, PA, United States). A constant flow (40 mL/min) of the mixture gas is sampled by a mass flow meter (Model 8200, Matheson, Basking Ridge, NJ, United States) and introduced into the plasma, while the excess gas is vented into the exhaust. This approach allows us to mix small concentrations of hydrogen into the helium gas. A stainless steel disk with a 0.5 mm orifice separates the plasma tube from the ionization chamber, increasing the pressure in the plasma tube.

The ionization chamber consists of a Swagelok tee downstream of the plasma tube. Ultrahigh purity nitrogen is introduced as the ionization gas into the ionization chamber using a mass flow controller (MKS Model 2468, Andover, MA, United States).

A single-quadrupole mass spectrometer (Flexar SQ300, PerkinElmer, Branford, CT, United States) is used to detect ions generated by PARCI. To couple the PARCI source, the counter-flow gas block of the mass spectrometer is removed and the original glass ion transfer capillary is replaced by a stainless steel capillary (6.35 mm o.d., 2.13 mm i.d., 17.78 cm length). The steel capillary is directly connected to the ionization tee. It should be noted that the larger i.d. of the stainless steel transfer capillary compared to the original glass capillary can adversely affect ion transfer efficiency from the capillary into the skimmer orifice. Nevertheless, we demonstrate in the Results and Discussion section that PARCI-MS has excellent sensitivity despite this initial simple design. Optimization of the capillary geometry would further improve the sensitivity in PARCI-MS and will be addressed in other reports.

Sample Preparation. Eight organobromine compounds, 1-bromobutane, 1,2-dibromoethane, 1-bromo-2,4-difluorobenzene, 2-bromo-3-methylthiophene, 2-bromo-4-methylpyridine, methyl bromoacetate, bromobenzene, and 2-bromotoluene (all from Sigma-Aldrich, St. Louis, MO, United States), are dissolved in high performance liquid chromatography (HPLC)-grade methanol (Sigma-Aldrich, St. Louis, MO, United States) at a concentration of ∼35 mM as stock solutions. Sample solutions are prepared by diluting stock solutions into desired concentrations using methanol.

Data Acquisition and Analysis. For quantitative analysis of brominated compounds with GC-PARCI-MS, the selected ion monitoring (SIM) mode is applied monitoring m/z 79 with a 100 ms pulse counting time and four samples per mass. Background ion intensities are measured in the absence of analytes by scanning m/z range 10 to 100.

All chromatograms are analyzed using OpenChrom software.[35] The start and end points of each chromatographic peak are manually selected. The baseline for each peak is defined as a straight line connecting the start and end points. The noise corresponding to each peak is determined by the standard deviation of the ion counts within 0.2 min before the start of each peak. The signal-to-noise (S/N) is calculated by dividing the peak height by the noise.

Safety Considerations. The microwave radiation from the cavity must be monitored to avoid exposure in the case of a radiation leak. The split line from the GC injector as well as the outlet of the mechanical pumps must be connected to proper exhaust lines to prevent the chemicals from entering the lab environment.

RESULTS AND DISCUSSION

Fundamental Investigations. Table 2 depicts the fundamental processes for analytical signal generation in PARCI for organobromines. In the first step, organobromines decompose within the plasma, quantitatively releasing bromine atoms in the form of HBr. In the second step, the resulting HBr is ionized in negative mode by mixing the flow from the plasma with a nitrogen flow directed into the ionization chamber. Helium metastable atoms ionize nitrogen and release electrons.[36] Ionization of HBr can then proceed via two possible mechanisms: (1) dissociative electron capture[37,38] and (2) proton transfer to a reagent ion, similar to negative mode chemical ionization.[39] The reagent ions arise from electron capture by species other than analyte. For example trace oxygen and nitrogen within the helium plasma gas lead to formation of oxygenated species such as NO_2^-, NO_3^-, and O_3^-, with NO_2^- being the most abundant ion. These species are also observed in other plasma-based ion sources such as corona discharge.[40,41] Another potential reagent ion observed in the spectra is Cl^-, which arises from chlorinated contaminants in the materials used for the construction of the ion source such as the tees.

Table 2. Two-Step Process for Formation of Br^- Ions from Organobromines in PARCI

step 1: major in-plasma reactions	step 2: electron generation and potential reactions for ionization
$R{-}Br \xrightarrow{H_2} HBr$	$He^* + N_2 \rightarrow N_2^+ + He + e$
$He + e \rightarrow He^* + e$	$HBr + e \rightarrow Br^- + H$
$\frac{1}{2}N_2 + O_2 \rightarrow NO_2$	$HBr + NO_2^- \rightarrow Br^- + HNO_2$

Considering the two-step process described above, hydrogen gas concentration and nitrogen gas flow rate constitute the two critical parameters impacting the analytical signal generation. Below, we present studies that investigate fundamentals of PARCI via variations in these parameters.

In-Plasma Reactions. Figure 2A compares the chromatogram obtained using GC-PARCI-MS in the absence of hydrogen reaction gas to that with 137 ppm (volume) H_2 added into the plasma gas. Five organobromine compounds with the concentration of 1 μM each are examined at a N_2 flow rate of 600 mL/min. The sensitivities (chromatographic peak heights) are improved 6- to 9-fold with the addition of H_2 reaction gas. The enhancement is larger for the late-eluting

dx.doi.org/10.1021/ac501964u | Anal. Chem. 2014, 86, 7954−7961

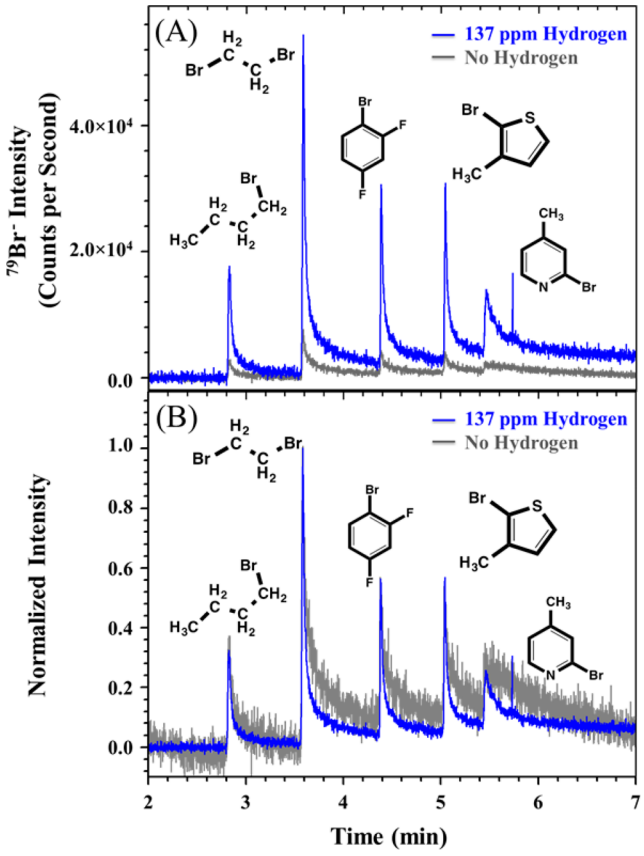

Figure 2. (A) Chromatograms obtained with and without reaction gas (H_2) in the plasma. A background value equivalent to average signal during 0.5 min prior to the first peak is subtracted from all intensities to superimpose the chromatograms. (B) Normalized chromatograms of panel A. The ionization gas flow rate was set at 600 mL/min for both experiments. Sample contains 1 μM of each compound.

compounds (higher boiling points) compared to the ones eluting earlier. Part of the enhancement stems from changes in the peak shapes as demonstrated in Figure 2B using normalized chromatograms. Peak tailing is reduced in the presence of hydrogen, with the largest improvement for high boiling point compounds. We attribute the peak tailing to deposition of the analytes on the walls of the plasma tube, leading to slower decomposition of the analytes and release of bromine. Note that plasma is not uniformly distributed across the tube, creating a temperature and reactive species concentration gradient from the center of the tube toward the walls. Analytes with higher boiling points are more likely to deposit on the cooler walls of the tube. Addition of hydrogen gas creates a sufficiently large concentration of hydrogen atoms, accelerating formation of HBr even from the analytes on the walls. In agreement with this analysis, we have observed that heating the ionization chamber and the transfer tube downstream of the plasma does not impact peak shapes, indicating that the compound-dependent tailing is mainly caused by deposition of analytes rather than the reaction product (HBr).

A second role of hydrogen addition is to buffer the composition of the plasma. This effect is more important for early eluting peaks because the residual solvent may change the plasma composition at the elution time of these compounds. Note that the solvent is not diverted in our studies. The hydrogen buffer effect is demonstrated in Figure 3 for 1,2-dibromoethane. The initial hold time in the GC temperature

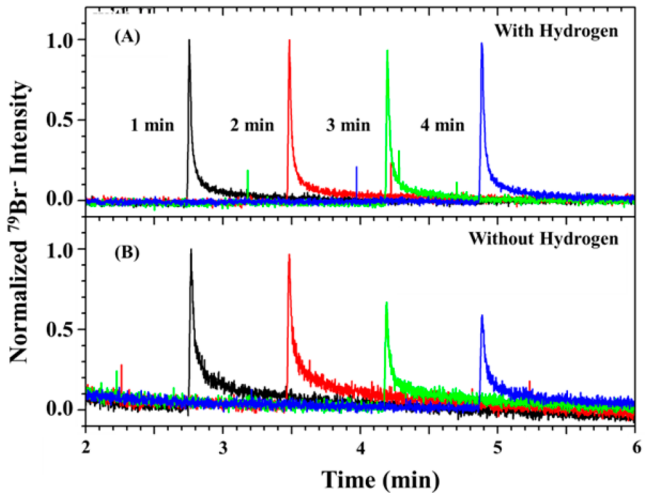

Figure 3. Buffer effect of reaction gas. (A) Helium plasma with hydrogen concentration at 137 ppm, (B) pure helium plasma. Intensities are normalized to the height of the first peak in each panel. The GC program for analytical performance (Table 1) with varying hold time at 35 °C was used. Nitrogen gas flow rate = 600 mL/min.

program is increased for each subsequent injection to delay the elution of the analyte. In the absence of hydrogen, the sensitivity gradually decreases with the hold time, suggesting that overlap with the residual methanol solvent improves sensitivity. Although an interesting trend, such a behavior is not analytically desirable. The variation in sensitivity is mitigated by addition of hydrogen into the plasma as shown in Figure 3.

Ionization Effects. The sensitivity improvement upon addition of hydrogen in Figure 2A cannot be explained solely based on peak shapes. For example, 1-bromobutane shows a minimal change in peak shape (Figure 2B) while its sensitivity is improved by a factor of 6 upon hydrogen addition. Accordingly, the majority of the enhancement is attributed to changes in ionization, the second step of signal generation in PARCI. To elucidate ionization effects, we have conducted a series of experiments to map the impact of hydrogen and nitrogen in their respective parameter spaces using a mixture of 1-bromobutane, 1,2-dibromoethane, methyl bromoacetate, 1-bromo-2,4-difluorobenzene, and 2-bromo-3-methylthiophene. For each experimental condition, a background spectrum is collected to characterize the potential reagent ions while the separation of brominated compounds is recorded by $^{79}Br^-$ single ion monitoring.

Impact of Hydrogen on Ionization. Figure 4 depicts 1-bromobutane's Br^- chromatographic peak area as well as ion intensities for Cl^- and NO_2^- (the major background ions) at various experimental conditions. Peak areas for other analytes as well as intensities for other background ions are shown in Figures S1 and S2 in the Supporting Information. We consider chromatographic peak areas rather than peak heights for investigation of ionization so that the changes in in-plasma reactions manifested in peak shapes do not complicate the analysis. Generally, the Br^- chromatographic peak areas (Figures 4A and S1, Supporting Information) increase up to 137 ppm of hydrogen followed by a decrease at higher hydrogen concentrations. This behavior is in stark contrast to that of NO_2^-, which shows a continuous decrease in intensity with hydrogen concentration, suggesting that NO_2^- does not serve as a regent ion for formation of Br^- from HBr.

dx.doi.org/10.1021/ac501964u | *Anal. Chem.* 2014, 86, 7954−7961

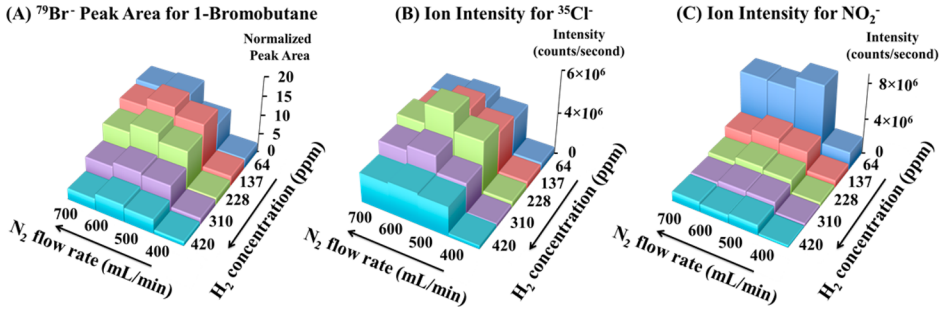

Figure 4. (A) Normalized Br^- chromatographic peak areas for 0.5 μL injection of 1 μM 1-bromobutane. All peak areas are normalized to the one obtained under H_2 concentration of 420 ppm and N_2 flow rate of 400 mL/min. (B) $^{35}Cl^-$ and (C) NO_2^- ion intensities as functions of reaction and ionization gas.

Importantly, all other oxygenated species (NO_3^-, O_2^-, and O_3^-) show a similar trend to that of NO_2^- with increasing hydrogen concentration (Figure S2, Supporting Information). Therefore, we conclude that addition of hydrogen to the plasma reduces the free oxygen available for formation of high electron-affinity neutral precursors of these ions (e.g., NO_2). Accordingly, the ionization of HBr is improved in the presence of moderate amounts of hydrogen because the competition for electrons from oxygenated species is reduced.

Trends in Figure 4 may also be used to infer the importance of proton transfer between Cl^- and HBr in formation of Br^-. Similar to Br^-, the intensity of Cl^- increases with moderate amounts of hydrogen. However, the intensity maximum for Cl^- occurs at higher hydrogen concentrations compared to Br^-. Moreover, the variation in Cl^- intensity with hydrogen concentration at each nitrogen flow rate occurs within a factor of 2, while the amount of Br^- ion varies up to a factor of 5 within the same experimental conditions. These observations suggest that Cl^- is also not likely to be a major reagent ion for HBr ionization at the current ionization conditions.

The observations above are in agreement with dissociative electron capture as the main ion formation mechanism for both background (NO_2^-, Cl^-) and analyte (Br^-) ions. With the introduction of hydrogen, competition from oxygenated species is reduced, giving rise to more efficient formation of halide ions. Higher hydrogen concentrations, however, reduce the metastable atom concentration in the plasma,[42] leading to a lower amount of electrons available for ionization and loss of sensitivity for all ions. These opposing factors give rise to an optimum hydrogen concentration for halide formation in 100–200 ppm range.

The higher optimum hydrogen setting for Cl^- compared to Br^- may be explained by considering concentration of chlorine-containing species reaching the ionization area. Unlike the chromatographic bands for brominated compounds, the chlorinated species originate from a continuous source of impurities and contaminants in the source. Hydrogen can promote release of chlorine from these compounds similar to the effect shown in Figure 2A for bromine. This effect partially compensates for the loss of ionization efficiency, shifting the maximum Cl^- ion intensity to higher hydrogen concentrations.

Effect of Nitrogen on Ionization. The effect of ionization gas flow rate on the Br^- chromatographic peak areas and background ion intensities are also presented in Figure 4. Generally, a rapid increase in the amount of all detected ions is observed up to the nitrogen flow rate of 500 mL/min. The changes above this flow rate are less drastic. Negative ion formation in PARCI relies on release of electrons via penning ionization of nitrogen (Table 2).[36] The flow of helium metastable atoms into the ionization area is mainly determined by the helium flow rate and plasma power, which are kept constant in the experiments. With increasing nitrogen flow rate, the pressure in the ionization area is elevated, leading to a faster reaction between metastable atoms and nitrogen. Accordingly, the concentration of electrons increases, resulting in faster electron capture and higher negative ion intensities. Moreover, ion transmission efficiency through the ion transfer capillary is expected to improve with increasing nitrogen flow rates. On the other hand, faster transmission times translate to less time available for electron capture. These opposing effects give rise to an optimum flow rate of nitrogen ~600 mL/min.

Analytical Performance of GC-PARCI-MS. The fundamental investigations above not only provide an understanding of analytical signal generation mechanisms but also reveal the optimum conditions for analytical measurements. To find the optimum operating conditions, the S/N values are normalized to the largest value for each compound within the parameter space for hydrogen and nitrogen. The normalized values are then averaged across five brominated compounds for each operating condition to create Figure S3 in the Supporting Information. The optimum conditions correspond to hydrogen concentration of 137 ppm and a nitrogen flow rate of 600 mL/min. The analytical performance of GC-PARCI-MS at this condition is presented below.

Compound-Independent Response Factor. A response factor independent of analytes' chemical structure is critical for an elemental quantification strategy. With a constant response factor, an elemental method can provide quantitative information in the absence of the individual standard for each analyte. To assess this characteristic for GC-PARCI-MS, we compared response factors for eight organobromines with significantly different chemical structures. To avoid the integration complications due to the tailing of the peaks discussed in fundamental studies, these eight compounds were injected into GC in two sets. Response factors were calculated via dividing the $^{79}Br^-$ peak area by the concentration of bromine corresponding to each compound.

Figure 5 illustrates the response factors normalized to the average response factor for the eight compounds. Triplet injections were carried out to assess the reproducibility of response factors. The relative standard deviations (RSDs) for all compounds were below 6% except for 2-bromo-4-methylpyridine, whose RSD was 13%. The large RSD is attributed to integration error caused by the peak tailing for this high-boiling point compound.

dx.doi.org/10.1021/ac501964u | *Anal. Chem.* 2014, 86, 7954–7961

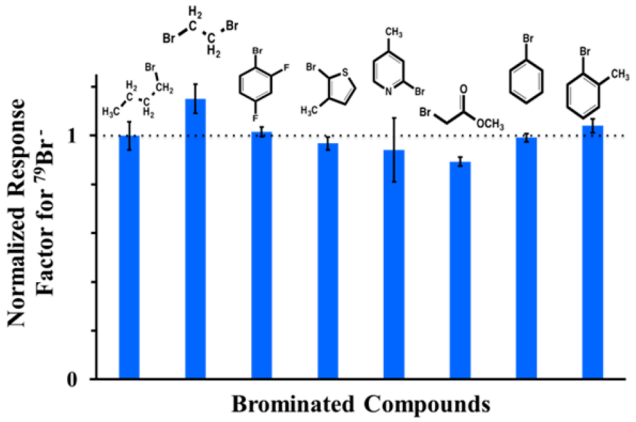

Figure 5. ^{79}Br response factor for brominated compounds normalized to the average response factor. 0.5 μL injections of a mixture containing 1 μM of each compound were carried out.

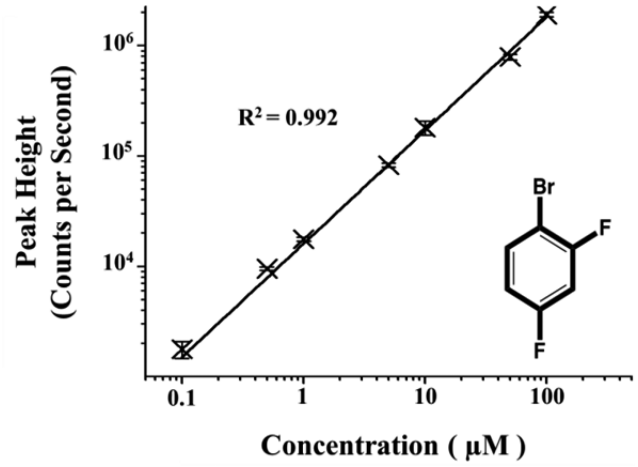

Figure 6. Response linearity based on peak height corresponding to 0.5 μL injections of 1-bromo-2,4-difluorobenzene with concentrations of 0.1 to 100 μM. Weighted least-squares fitting is applied to calculate the best fit.

A normalized response factor of 1 is ideal for quantification. The majority of the analytes show close to ideal behaviors in Figure 5. Deviations up to 15% are observed, which may be the result of sample introduction biases within the split injector (e.g., decomposition) and integration biases caused by tailing. The relatively uniform response factors demonstrate the potential of GC-PARCI-MS for quantification in the absence of compound-specific standards. This characteristics arise from complete reaction of brominated compounds within the plasma, leading to quantitative release of bromine for subsequent ionization.

Dynamic Range and Limits of Detection. Detection limits depend on chromatographic peak shape and noise levels prior to each peak. Therefore, slight variations in detection limits between compounds are expected even with a constant response factor based on peak area. 1-Bromo-2,4-difluorobenenze eluting in the middle portion of the chromatograms is selected as a representative to demonstrate the dynamic range and limits of detection.

0.5 μL samples of 1-bromo-2,4-difluorobenenze with the concentrations ranging from 0.1 to 100 μM were injected into the GC-PARCI-MS. The calibration curve based on average peak heights for triplicate injections is shown in Figure 6. Weighted least-squares fitting of the peak heights was performed using a weighting factor of $1/(SD)^2$. A linear response with r^2 of 0.992 is observed over at least 3 orders of magnitude. Using peak areas, a linear response with r^2 of 0.983 is observed over the same concentration range (Figure S4, Supporting Information). The lower linearity is attributed to integration errors due to peak tails.

For a comparison of sensitivities in PARCI-MS and ICP-MS, we consider the on-column amount of bromine entering the ion source rather than the total injected amount into the GC. This approach eliminates sample introduction variation arising from different injection methods, reflecting ionization and ion transfer efficiencies. In our studies, injecting 0.5 μL of 0.1 μM 1-bromo-2,4-difluorobenenze results in 1 fmol of bromine entering PARCI, considering the split ratio of 50:1 in the injector. The S/N ratio corresponding to this injection is 8.3. Thus, the detection limit of GC-PARCI-MS is estimated to be 0.36 fmol Br (29 fg). Compared with a detection limit of around 100−150 fg bromine on column using GC-ICP-MS,[24,25,43] an almost 4-fold improvement in the detection limit is estimated for organobromine analysis using GC-PARCI-MS. Note that this detection limit is observed with the tailing of the peaks. Accordingly, resolving the peak tailing in PARCI is expected to further increase the peak heights and the sensitivity. Moreover, similar to ICP-MS, the overall method detection limits for PARCI-MS can be improved by utilizing splitless injection where all of the injected analyte is introduced into the ion source.

CONCLUSIONS

The effects of two critical parameters in PARCI, reaction gas (H_2) and ionization gas (N_2), reveal in-plasma reactions followed by electron capture as the main mechanism for formation of Br^- from organobromines. The moderate amounts of hydrogen accelerate bromine release from the organic compounds within the plasma and reduce the ionization competition from oxygenated species, leading to better sensitivities. However, higher amounts of hydrogen degrade sensitivity mainly via reduction of helium metastable atom concentration. The effect of nitrogen is largely manifested in the second step of signal generation. An optimum flow of nitrogen is needed to rapidly quench the helium metastable atoms, providing high concentration of electrons for ionization while allowing sufficient time for effective electron capture during transit to the MS. This electron capture mechanism is efficient for Br detection, providing better sensitivities compared to ICP-MS. Fundamental investigations and analytical performance of PARCI for other halogens will be discussed in future reports. Moreover, PARCI-MS sensitivities may be further improved by optimization of ion transfer capillary geometry, particularly the exit orifice size.

We have demonstrated that PARCI-MS provides a relatively uniform response factor for bromine detection, enabling quantification based on bromine content without the need for compound-specific standards. This capability is particularly useful for discovery-based studies such as metabolite profiling in early drug development and environmental screening where standards may not be readily available. One current limitation of PARCI in this area is the tailing in the chromatographic peaks observed under the current operating conditions. The peak tails lead to integration errors in peak areas, lower peak heights because of peak broadening, and compromise

dx.doi.org/10.1021/ac501964u | *Anal. Chem.* 2014, 86, 7954−7961

separation power due to peak overlapping. Our investigations have shown that the tailing is a consequence of analyte deposition on the walls of the plasma tube. Therefore, the use of high-power plasmas with higher gas kinetic temperature is expected to resolve this limitation, further improving the analytical performance of PARCI.

Argon-based isobaric interferences create a challenge for Br analysis in ICP-MS, especially for quadrupole instruments without reaction and collision cells. Ionization in negative mode in PARCI alleviates the challenges associated with these isobaric interferences. Moreover, unlike ICP, PARCI can be easily interfaced with readily available atmospheric pressure sampling mass spectrometers. The presented studies have been performed on an instrument originally configured for electrospray ionization with minimal modifications. This compatibility allows use of high-performance mass spectrometers with better ion transmission and ion separation capabilities (e.g., high resolution and MS/MS) to further improve the analytical figures of merit. Finally, PARCI offers the possibility of obtaining elemental and molecular information using one instrument.

■ ASSOCIATED CONTENT

Ⓢ Supporting Information

Normalized $^{79}Br^-$ chromatographic peak areas in various operating conditions for four organobromines, background ion intensities at various operating conditions, average normalized signal-to-noise ratios for five organobromines as a function of operating parameters, and bromine response linearity based on chromatographic peak areas. This material is available free of charge via the Internet at http://pubs.acs.org.

■ AUTHOR INFORMATION

Corresponding Author

*K. Jorabchi. E-mail: kj256@georgetown.edu. Phone: 202-687-2066.

Notes

The authors declare no competing financial interest.

■ ACKNOWLEDGMENTS

This work is supported by Georgetown University and PerkinElmer Inc. We are grateful to PerkinElmer Inc. for the loan of a SQ300 instrument. We are thankful to Dr. Jack Syage of Syagen Technology for providing the microwave power supply.

■ REFERENCES

(1) Covaci, A.; Harrad, S.; Abdallah, M. A.-E.; Ali, N.; Law, R. J.; Herzke, D.; de Wit, C. A. *Environ. Int.* **2011**, *37*, 532−556.
(2) Richardson, S. D.; Ternes, T. A. *Anal. Chem.* **2014**, *86*, 2813−2848.
(3) Costa, L. G.; Giordano, G. *Neurotoxicology* **2007**, *28*, 1047−1067.
(4) Dingemans, M. M.; van den Berg, M.; Westerink, R. H.; Dingemans, M.; van den Berg, M.; Westerink, R. *Environ. Health Perspect.* **2011**, *119*, 900.
(5) Cuyckens, F.; Balcaen, L. I.; De Wolf, K.; De Samber, B.; Van Looveren, C.; Hurkmans, R.; Vanhaecke, F. *Anal. Bioanal. Chem.* **2008**, *390*, 1717−1729.
(6) Elder, D.; Lipczynski, A.; Teasdale, A. *J. Pharm. Biomed. Anal.* **2008**, *48*, 497−507.
(7) Ballesteros-Gómez, A.; de Boer, J.; Leonards, P. E. *Anal. Chem.* **2013**, *85*, 9572−9580.
(8) Ballesteros-Gómez, A.; Brandsma, S.; de Boer, J.; Leonards, P. *Anal. Bioanal. Chem.* **2014**, *406*, 2503−2512.
(9) Ho, K.-L.; Murphy, M. B.; Wan, Y.; Fong, B. M.-W.; Tam, S.; Giesy, J. P.; Leung, K. S.-Y.; Lam, M. H.-W. *Anal. Chem.* **2012**, *84*, 9881−9888.
(10) Feo, M. L.; Barón, E.; Aga, D. S.; Eljarrat, E.; Barceló, D. *J. Chromatogr. A* **2013**, *1301*, 80−87.
(11) Stapleton, H. M.; Allen, J. G.; Kelly, S. M.; Konstantinov, A.; Klosterhaus, S.; Watkins, D.; McClean, M. D.; Webster, T. F. *Environ. Sci. Technol.* **2008**, *42*, 6910−6916.
(12) González-Gago, A.; Marchante-Gayón, J. M.; Ferrero, M.; Alonso, J. I. G. *Anal. Chem.* **2010**, *82*, 2879−2887.
(13) Muller, A. L.; Mello, P. A.; Mesko, M. F.; Duarte, F. A.; Dressler, V. L.; Muller, E. I.; Flores, E. M. *J. Anal. At. Spectrom.* **2012**, *27*, 1889−1894.
(14) Popp, M.; Hann, S.; Koellensperger, G. *Anal. Chim. Acta* **2010**, *668*, 114−129.
(15) Profrock, D.; Prange, A. *Appl. Spectrosc.* **2012**, *66*, 843−868.
(16) Clough, R.; Harrington, C. F.; Hill, S. J.; Madrid, Y.; Tyson, J. F. *J. Anal. At. Spectrom.* **2013**, *28*, 1153−1195.
(17) Houk, R. *Anal. Chem.* **1986**, *58*, 97A−105A.
(18) Egorova, T.; Dietiker, R.; Hattendorf, B.; Günther, D. *Spectrochim. Acta, Part B* **2012**, *76*, 40−47.
(19) Gammelgaard, B.; Jensen, B. P. *J. Anal. At. Spectrom.* **2007**, *22*, 235−249.
(20) Mingwu, S.; Chao, W.; Yongjuan, J.; Xinhua, D.; Xiang, F. *Anal. Chem.* **2010**, *82*, 5154−5159.
(21) Bierla, K.; Riu, A.; Debrauwer, L.; Zalko, D.; Bouyssiere, B.; Szpunar, J. *J. Anal. At. Spectrom.* **2010**, *25*, 889−892.
(22) Andra, S. S.; Makris, K. C.; Shine, J. P.; Lu, C. *Environ. Int.* **2012**, *38*, 45−53.
(23) Meermann, B.; Bockx, M.; Laenen, A.; Van Looveren, C.; Cuyckens, F.; Vanhaecke, F. *Anal. Bioanal. Chem.* **2012**, *402*, 439−448.
(24) Novak, P.; Zuliani, T.; Milačič, R.; Ščančar, J. *Anal. Chim. Acta* **2014**, *827*, 64−73.
(25) Swarthout, R. F.; Kucklick, J. R.; Davis, W. C. *J. Anal. At. Spectrom.* **2008**, *23*, 1575−1580.
(26) Medina, C.; Pitarch, E.; López, F.; Vázquez, C.; Hernández, F. *Anal. Bioanal. Chem.* **2008**, *390*, 1343−1354.
(27) Meyer, C.; Muller, S.; Gurevich, E. L.; Franzke, J. *Analyst* **2011**, *136*, 2427−2440.
(28) Na, N.; Zhao, M. X.; Zhang, S. C.; Yang, C. D.; Zhang, X. R. *J. Am. Soc. Mass Spectrom.* **2007**, *18*, 1859−1862.
(29) Kunze, K.; Miclea, M.; Franzke, J.; Niemax, K. *Spectrochim. Acta, Part B* **2003**, *58*, 1435−1443.
(30) Li, W.; Zheng, C. B.; Fan, G. Y.; Tang, L.; Xu, K. L.; Lv, Y.; Hou, X. D. *Anal. Chem.* **2011**, *83*, 5050−5055.
(31) Li, Y.; Hu, J.; Tang, L.; He, Y.; Wu, X.; Hou, X.; Lv, Y. *J. Chromatogr. A* **2008**, *1192*, 194−197.
(32) Guchardi, R.; Hauser, P. C. *J. Anal. At. Spectrom.* **2004**, *19*, 945−949.
(33) Brede, C.; Pedersen-Bjergaard, S.; Lundanes, E.; Greibrokk, T. *J. Anal. At. Spectrom.* **2000**, *15*, 55−60.
(34) Wang, H. P.; Lin, N. H.; Kahen, K.; Badiei, H.; Jorabchi, K. *J. Am. Soc. Mass Spectrom.* **2014**, *25*, 692−695.
(35) Wenig, P.; Odermatt, J. *BMC Bioinf.* **2010**, *11*, 405.
(36) Richardson, W.; Setser, D. *J. Chem. Phys.* **2003**, *58*, 1809−1825.
(37) Adams, N. G.; Smith, D.; Viggiano, A.; Paulson, J. F.; Henchman, M. J. *J. Chem. Phys.* **1986**, *84*, 6728−6731.
(38) Fedor, J.; May, O.; Allan, M. *Phys. Rev. A* **2008**, *78*, 032701.
(39) Veres, P.; Roberts, J. M.; Warneke, C.; Welsh-Bon, D.; Zahniser, M.; Herndon, S.; Fall, R.; de Gouw, J. *Int. J. Mass Spectrom.* **2008**, *274*, 48−55.
(40) Skalny, J. D.; Mikoviny, T.; Matejcik, S.; Mason, N. J. *Int. J. Mass Spectrom.* **2004**, *233*, 317−324.
(41) Nagato, K.; Matsui, Y.; Miyata, T.; Yamauchi, T. *Int. J. Mass Spectrom.* **2006**, *248*, 142−147.
(42) Wright, J. P.; Heywood, M. S.; Thurston, G. K.; Farnsworth, P. B. *J. Am. Soc. Mass Spectrom.* **2013**, *24*, 335−340.

(43) Wilbur, S.; Soffey, E. *Handbook of Hyphenated ICP-MS Applications*, 2nd ed.; Agilent Technologies: Santa Clara, CA, 2007; p 40.